Supporting Information

S, O dual-doped porous carbon derived from activation of waste papers as electrodes for high performance lithium ion capacitors

Jian Hao[a], Bai Jun[a], Xiu Wang[a], Yanxia Wang[a], Qingjie Guo[a], Yu Yang[b] , Jiupeng Zhao[b], Caixia Chi [b], and Yao Li[c]*

[a] State Key Laboratory of High-efficiency Utilization of Coal and Green Chemical Engineering, College of Chemistry & Chemical Engineering, Ningxia University, Yinchuan 750021, China

E-mail: haojian2017@126.com

[b] School of Chemistry and Chemical Engineering, Harbin Institute of Technology, 150001, Harbin, China

[c] Center for Composite Materials, Harbin Institute of Technology, 150001, Harbin, China

Table S1. XPS analysis of the samples

Sample	C (at%)	O (at%)	S (at%)	N (at%)
S-NPC-40	88.49	9.05	2. 13	0.33
S-NPC-60	88.10	9.51	2.08	0.31
S-NPC-KOH	89.31	7.97	2.33	0.39
S-NPC-40 without H_2SO_4 solvothermal	88.69	10.09	0.76	0.46

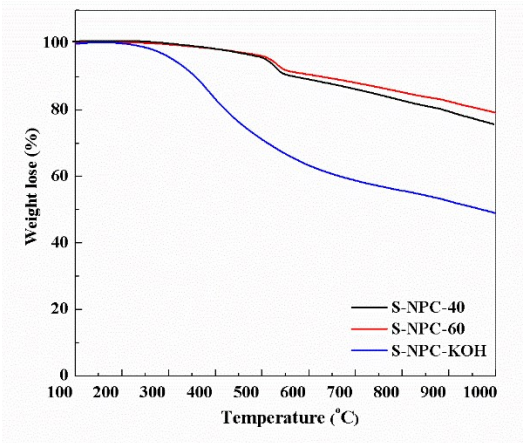

Fig. S1 TGA results of S-NPC-40, S-NPC-60 and S-NPC-KOH under N_2.

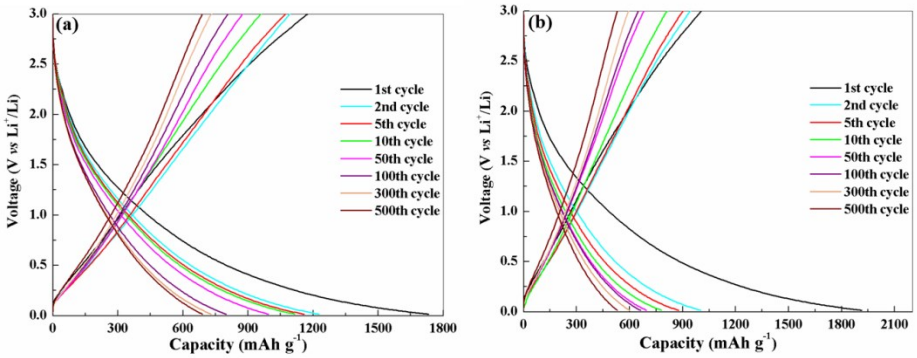

Fig. S2 Charge-discharge curves of the S-NPC-60 and S-NPC-KOH anode at a current density of 0.1 A g^{-1}.

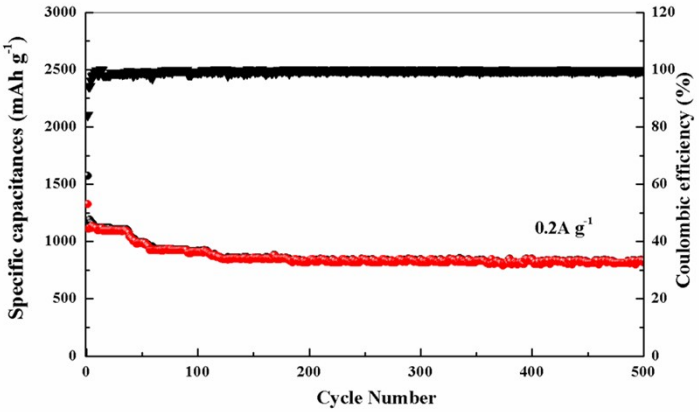

Fig. S3 Cycle performance of the S-NPC-40 anode at

a current density of 0.2 A g^{-1} for 2000 cycles.

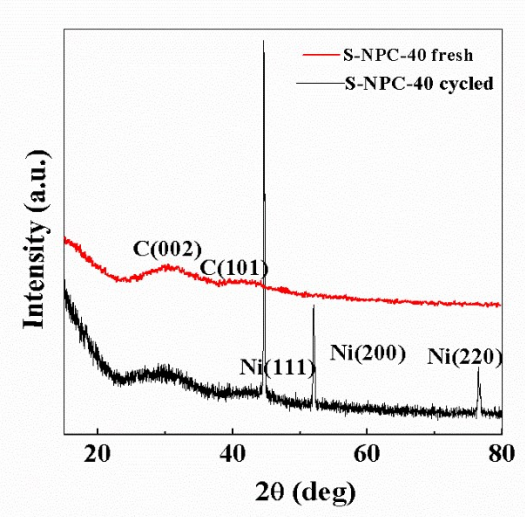

Fig. S4 XRD patterns of S-NPC-40 samples before and after cycling.

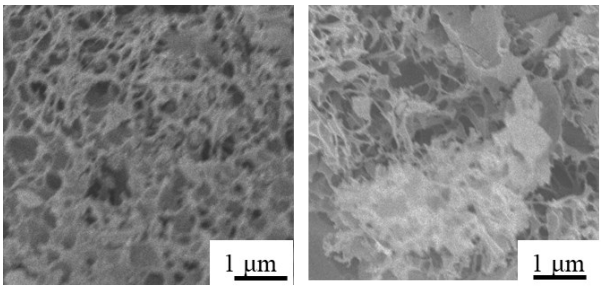

Fig. S5 A typical SEM image of S-NPC-40 anode and cathode after cycling.

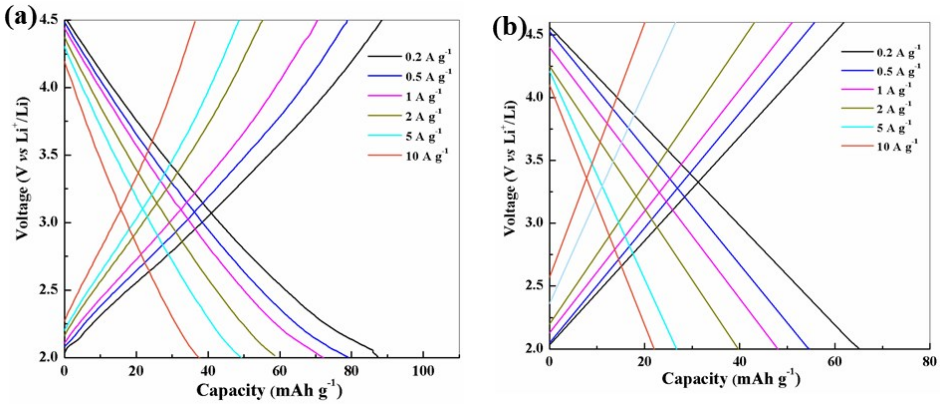

Fig. S6 Charge-discharge curves of the S-NPC-60 and S-NPC-KOH cathode at different current densities.

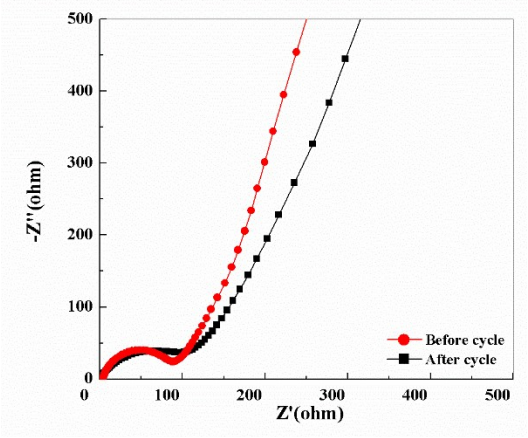

Fig. S7 Nyquist plots of S-NPC-40 before and after cycling.

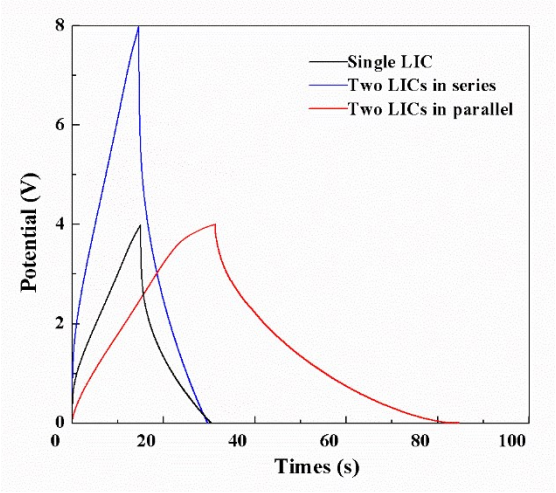

Fig. S8 GCD curves of single S-NPC-40//S-NPC-40 LIC, two S-NPC-40//S-NPC-40 LICs in parallel, and two S-NPC-40//S-NPC-40 LICs connected in series.